ACS APPLIED MATERIALS & INTERFACES

Research Article

www.acsami.org

# Integrins-FAK-Rho GTPases Pathway in Endothelial Cells Sense and Response to Surface Wettability of Plasma Nanocoatings

Yang Shen,[†,∥] Yunlong Ma,[†,∥] Min Gao,[†] Yi Lai,[†] Guixue Wang,[‡] Qingsong Yu,[§] Fu-zhai Cui,[⊥] and Xiaoheng Liu*[,†]

[†]Institute of Biomedical Engineering, School of Preclinical and Forensic Medicine, Sichuan University, Chengdu 610041, China

[‡]Key Laboratory of Biorheological Science and Technology, Ministry of Education, Bioengineering College, Chongqing University, Chongqing, 400030, China

[§]Center for Surface Science and Plasma Technology, Department of Mechanical and Aerospace Engineering, University of Missouri, Columbia, Missouri 65211, United States

[⊥]State Key Laboratory of New Ceramics and Fine Processing, Department of Material Science and Engineering, Tsinghua University, Beijing 100084, China

Supporting Information

**ABSTRACT:** Vascular endothelial cell (EC) adhesion and migration are essential processes in re-endothelialization of implanted biomaterials, which are affected by surface properties of implanted materials such as surface wettability. Our previous study demonstrated that, as model substrates, EC adhesion/migration showed an opposite behavior on the hydrophobic and hydrophilic surfaces of plasma $SiO_x$:H nanocoatings. Extending our previous works, the expression and distribution of crucial proteins in integrins-FAK-Rho GTPases signaling pathways were examined, respectively. The results showed that a hydrophilic surface could enhance the expression of focal adhesion protein associated with cell adhesion; however, the hydrophobic surface could improve the expression of Rho GTPases associated with cell migration and phosphorylation level of FAK, revealing the potential reason of surface wettability mediating different cells' adhesion/migration behaviors. These findings reveal the relationship and molecular mechanism of endothelial cell adhesion/migration, which was expected to guide the surface modification of implants for accelerating endothelialization.

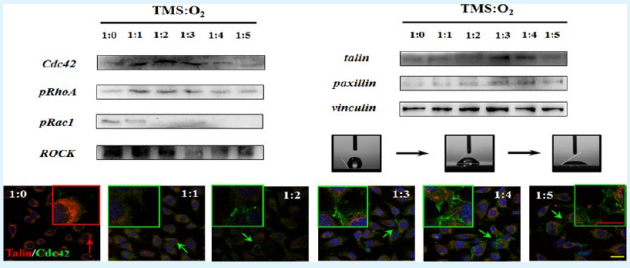


**KEYWORDS:** *plasma nanocoating, surface wettability, cell adhesion/migration, focal adhesion, FAK, Rho GTPases*

## 1. INTRODUCTION

The behavior of surface/interface between biomaterials and cell/tissue is a key factor to determine biocompatibility of implanted materials. In particular, with regard to coronary stents, many reports have suggested metal stents could induce thrombogenicity and allergenicity, and then result in acute thrombus and in-stent restenosis (ISR).[1] Rapid re-endothelialization was regarded as the best way to improve the hemocompatibility, and inhibit acute thrombus and ISR.[2] During the course of re-endothelialization, the neighboring vascular endothelial cells (ECs) migrating on a stent surface is the main process of re-endothelialization after stent implantation.[2,3] In addition, increasing evidence showed that endothelial progenitor cells (EPCs) from circulatory blood also contributed to vascular repair and stent re-endothelialization.[4,5] Therefore, the proper surface of coronary stents should be designed and modified in favor of EC adhesion and migration.

Nowadays, many techniques have been applied for surface modification of coronary stents, and researchers have found various surface properties could affect cell adhesion behaviors, including surface roughness and micro-patterns,[3] surface chemistry and wettability,[6] and charge distribution.[7] Among these properties of implanted biomaterials, surface wettability (surface hydrophilicity/hydrophobicity) is a major surface parameter in determining protein adsorption and cell–biomaterial interaction in vitro and in vivo.[8]

However, few works focusing on cell migration contribute to reendothelization. There is no clear relationship and relative mechanism between EC adhesion and migration behavior in response to surfaces of implanted materials. EC adhesion and migration are essential processes in re-endothelialization of implanted biomaterials, which are involved in intracellular cytoskeleton rearrangement. Focal adhesion (FA) formation and disassembly drives the migration cycle by activating Rho GTPases which regulate actin polymerization and myosin II activity.[9] This process is controlled by integrin, which is a family of extracellular matrix (ECM) receptors regulating many aspects of cell behavior, in particular cell adhesion and

Received: March 17, 2013
Accepted: May 5, 2013
Published: May 5, 2013

   dx.doi.org/10.1021/am400973a | ACS Appl. Mater. Interfaces 2013, 5, 5112–5121

migration. Around activated integrin clusters, cytoskeletal proteins as the ligands of $\beta$ integrin cytoplasmic tails assemble together to form FA plaques.[10] Among these FA complex proteins, intracellular talin, paxillin, and vinculin are the most essential cytoskeletal proteins which provide enough supports for cell adhesion. The integrin-binding proteins talin and paxillin recruit vinculin to focal contacts, which mediated focal adhesion kinase (FAK) activation via C-terminal focal-adhesion targeting domain. The initial phosphorylation of Y397 tyrosine of FAK, serving as a scaffold or adaptor, becomes a binding site and recruits a number of structural and signaling molecules for the SH2 domain of Src family kinases and phosphatidylinositol-3 kinase (PI3K), which leads to a cascade of activation of other downstream signaling pathways.[11] The PI3K signaling pathway is an important regulator of ECs functions including cell survival and proliferation, as well as cell migration.[12] AKT, a serine/threonine protein kinase (also called protein kinase B, PKB), is recruited to the cell membrane and phosphorylated by its binding to PI3K. The phosphorylation of AKT subsequently activates eNOS-NO and Rho-family GTPases events, and eventually induces cell migration. Numerous opportunities for signal integration and crosstalk exist between Rho GTPases and PI3K mediating signaling pathways.

Rho-family GTPases (RhoA, Rac1 and Cdc42) could result in direct local actin assembly to form stress fibres, lamellipodia or filopodia, respectively. The activated RhoA, Rac1, and Cdc42 act together to control cytoskeleton dynamics, and determine cell motility eventually.[13] Therefore, cell adhesion and migration on the surface of material possibly depends on intercellular FA formation and activation of Rho-family GTPases, and the associated cellular FAK signaling events.

In our previous study,[14] the plasma $SiO_x$:H nanocoating with different wettability was used to explore the effects of surface wettability on cell adhesion and migration. The results indicated that EC adhesion/migration showed opposite behavior on the hydrophilic and hydrophobic surfaces, which is consistent with most researchers' conclusions;[6,8,15] however, hydrophobic surfaces (98.5+2.3° to 82.3+3.5°) could promote EC migration compared with hydrophilic surfaces. We also found that EC migration on hydrophilic/hydrophobic surfaces of plasma $SiO_x$:H nanocoatings was all dependent on phosphorylation of FAK, and determined in part by the expression and distribution of multiple proteins. These differences led us to further examine possible molecular mechanism of surface wettability regulating cell behavior. Accordingly, the expression and distribution of the intracellular crucial proteins in integrin-FAK-Rho GTPases signaling pathway to various surface wettabilities were studied in the present study, to make clear the integrin-FAK associated signaling pathway involved in surface-induced endothelial cell adhesion and migration. These findings reveal the relationship and mechanism of endothelial cell adhesion/migration, which was expected to guide the design of implant surface for accelerating endothelialization.

## 2. METHODS

**Plasma Nanocoating and Surface Characterization.** As model substrates with different wettability, the $SiO_x$:H nanocoatings were deposited on ultra-flat silicon wafers (6.082−12.55 Ω cm in resistivity, *p*-type with Boron as dopant, site flatness specification ≤0.05 $\mu$m, Silicon Valley Microelectronics, Inc., Santa Clara, CA 95051, U.S.A.) by a low-temperature plasma deposition technique. The plasma nanocoated wafers with 1 × 5 cm were directly used to culture cells and collect proteins for western blot analysis without any fibronectin (FN) or collagen (Col) precoating.

Low-temperature plasma deposition technique was performed at the Center for Surface Science and Plasma Technology in the University of Missouri (Columbia, MO, U.S.A.). The silicon wafers were pretreated with oxygen plasma for 2 min for cleaning. Subsequently, plasma $SiO_x$:H nanocoatings were deposited in a mixture of TMS (1 sccm) and oxygen (from 0 sccm to 5 sccm, respectively) under conditions of 25 mtorr and 5 W of dc power input. The deposition duration was controlled at 1.5−7 min to adjust the thickness of plasma $SiO_x$:H nanocoatings (the thickness of coatings in all groups were adjusted at 30−40 nm) . The sample identification codes and preparation conditions used in this study were summarized in Table 1. The plasma coating thickness was detected by a null-seeking type AutoEL-II Automatic Ellipsometer (Rudolph Research Corporation, Flanders, NJ) with a 632.8 nm helium−neon laser light source. The surface wettability of plasma coated film was assessed using a contact angle measurement system (VCA 2500XE, U.S.A.).

**Table 1. Preparation Conditions of Plasma $SiO_x$:H and Surface Characterization**

| identification codes of samples | flow ratio of TMS and $O_2$ | contact angle | deposition duration (min) | thickness (nm) |
|---|---|---|---|---|
| 1:0 | TMS : $O_2$ = 1 sccm:0 sccm | 98.5±2.3° | 1.5 | 40.65±1.01 |
| 1:1 | TMS : $O_2$ = 1 sccm:1sccm | 82.3±3.5° | 2 | 31.36±1.02 |
| 1:2 | TMS : $O_2$ = 1 sccm:2 sccm | 47.5±3.0° | 3 | 34.02±0.87 |
| 1:3 | TMS : $O_2$ = 1 sccm:3 sccm | 41.5±3.0° | 5 | 31.14±0.81 |
| 1:4 | TMS : $O_2$ = 1 sccm:4 sccm | 29.3±2.5° | 6 | 35.78±0.63 |
| 1:5 | TMS : $O_2$ = 1 sccm:5 sccm | 26.3±4.0° | 7 | 35.21±0.78 |

**Cell Culture.** Because of their higher affinity to the materials surfaces, human vascular endothelial cell lines, EA.hy 926 cells were used in this study instead of primary endothelial cells, which are hybridoma cell lines between human umbilical vein endothelial cells (HUVECs) and the epithelioma A549 cells, and retain most features of HUVECs, including the expression of endothelial adhesion molecules and human factor VIII-related antigen. It has been identified in previous works in our laboratory. EA.hy 926 cells were cultured in RPMI1640 medium (Invitrogen Company, U.S.A.) supplemented with 10% fetal bovine serum, and were maintained in a 5% $CO_2$ incubator at 37°C. Cells were seeded at concentration of 1,000 cells/mm$^2$ on $SiO_x$:H plasma nanocoated wafers.

**Western Blot Analysis.** After 48 h culture, cells on each wafer (1×5 cm) with 60−80% confluence were washed three times with PBS and disintegrated by 50 $\mu$L cell lysis solution containing 1% Phenylmethanesulfonyl fluoride and protease inhibitor. The total proteins were collected and centrifuged with 10,000 rpm at 4 °C for 5−10 min. Equal amounts of protein were loaded onto each lane of a 12% SDS-PAGE gel. After blotting, polyvinylidene difluoride membranes (PVDF, GE Healthcare) were blocked for 2 h in 3% BSA in TBST buffer (20 mmol/L Tris-HCl [pH 8.0], 150 mmol/L NaCl, 0.05% Tween 20) at 37 °C. Membranes were then incubated

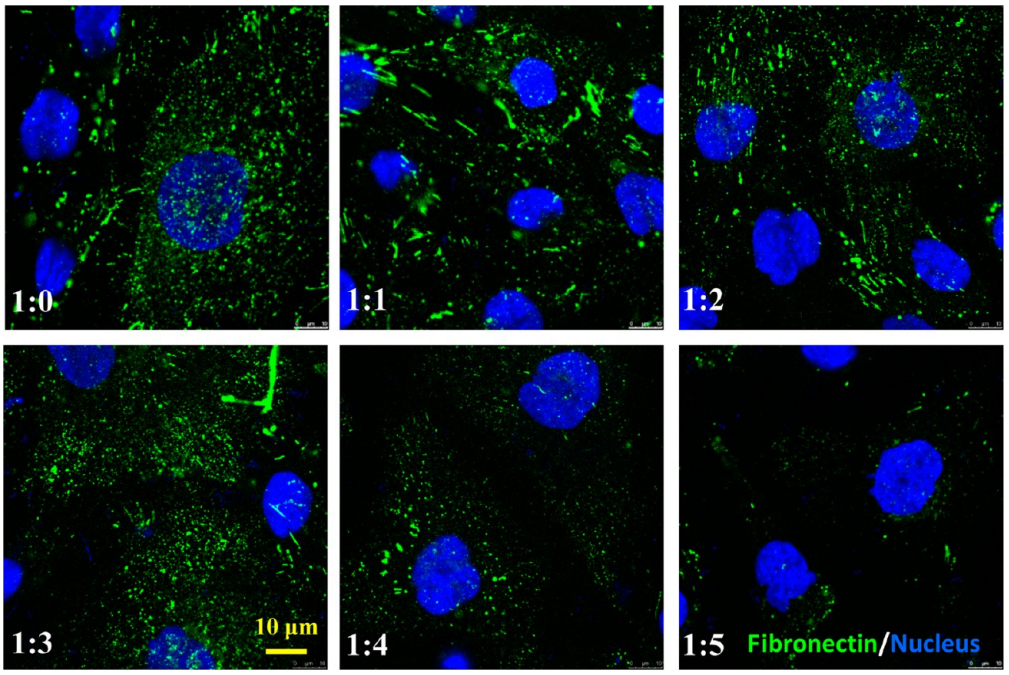


**Figure 1.** Fibronectin distribution on the plasma coated silicon wafers with various surface wettabilities to support cells adhesion. Fibronectin (green) was incubated with primary antibody, and stained by FITC labeled second antibody, nucleus were stained by DAPI (blue). Scale bar represents 10 $\mu$m.

with primary antibodies overnight at 4 °C. The binding of secondary HRP antibodies was visualized by enhanced chemiluminescence. Images of bands were determined using Molecular Image ChemiDoc XRS$^+$ with Image Lab Software. The tests were performed three times at least, and quantification was performed and analyzed by Image J 1.44p software (National Institutes of Health, U.S.A.). Double intrinsic controls ($\beta$-actin and GAPDH) were used to guarantee the uniformity of equally loaded protein among all groups. The detailed information of primary antibodies and secondary antibodies are as follows.

The primary antibodies of integrins subunits, including anti-integrin $\alpha$V (H-2) mouse mAb (sc-376156), anti-integrin $\beta$1 (A-4) mouse mAb (sc-374429), and anti-integrin $\beta$3 (B-7) mouse mAb (sc-466655); the primary antibodies of FA complexes, including anti-vinculin (G-11) mouse mAb (sc-55465), anti-talin (8D4) mouse mAb (sc-59881), anti-paxillin (D-9) mouse mAb (sc-365174); the primary antibodies of (*p*)FAK, including anti-FAK (A-17) rabbit mAb (sc-1688), anti-*p*FAK (2D11) mouse mAb (against a phosphopeptide corresponding to amino acid residues surrounding tyrosine 397 of FAK of human origin, sc-81493); the primary antibodies of PI-3K and (*p*)AKT, including anti-PI3K mouse mAb (sc-100407), anti-*p*AKT rabbit mAb (sc135650) and anti-AKT1 rabbit mAb (sc-271149); the primary antibodies of small G proteins, including anti-*p*Rac1 (Ser 71) rabbit mAb (sc-12924-R), anti-*p*RhoA (Ser 188) rabbit mAb (sc-32954) were purchased from Santa Curz Biotechnology, Inc (CA, U.S.A.). Only anti-Cdc42 rabbit mAb(ab64533) and anti-ROCK rabbit mAb (ab45171) were purchased from Abcam, Inc. (Cambridge, U.K.). The loading controls, $\beta$-actin and GAPDH were obtained from Dingguo Biotechnology Co., LTD (Beijing, China). The peroxidase-conjugated goat anti-mouse IgG and goat anti-rabbit IgG (secondary antibody) were purchased from Dingguo Biotechnology Co., LTD (Beijing, China).

**Immunofluorescence Assay.** After 48 h cell culture (equal to culture duration of western blot analysis), cells were fixed with 4% paraformaldehyde and permeabilized with 0.3% Triton X-100 for 10 min. Following fixation and permeabilization, samples were blocked by adding 1% (w/v) bovine serum albumin for 15 min at room temperature. Cells were incubated in the primary antibody solution (1:100 dilution, Santa Cruz, U.S.A.) at 4°C overnight. Each step was followed by washing with PBS for 5 min for three times. The secondary FTIC-conjugated immunoglobulin (Goat anti-mouse IgG, green color fluorescence) or PE-conjugated immunoglobulin (Goat anti-rabbit IgG, red color fluorescence) were purchased from Biosynthesis biotechnology Co., LTD (Beijing, China), and AMCA-conjugated goat anti-rabbit IgG (blue fluorescence) were purchased from Cali-Bio, Inc. (Coachella, CA, U.S.A.). The fluorescent labeled secondary antibodies were incubated with respective primary antibody for 60 min. Then, the DAPI (4′,6′-diamidino-2-phenylindole) with 1:800 dilution was added for nuclei staining for 30 min. Samples were sealed by 10% glycerol, kept in a dark place, and observed by laser scanning confocal microscopy (Leica TCS SP5, Germany).

For the double staining, two primary antibody solution (anti-rabbit mAb and anti-mouse mAb) were diluted 1:200 with PBS, mixed and incubated with cells at 4°C overnight, the secondary FTIC-conjugated immunoglobulin and PE-conjugated immunoglobulin were also diluted 1:100 with PBS, mixed and incubated at 37°C for 60 min to conjugate respective primary antibody. For the FAK and *p*-FAK double staining, the primary antibody, anti-*p*FAK (2D11) mouse mAb was firstly incubated with cells at 37°C for 3 h (for conjugate phosphorylation sites of FAK prior to total FAK), then second primary antibody, anti-FAK (A-17) rabbit mAb (sc-1688), were added and incubated with cells.

**Statistical Analysis.** The data obtained in this study were analyzed by using statistical software SPSS 11.5 (SPSS, Inc., Chicago, Illinois) and reported as the means ± standard error.

Data obtained from different treatment groups were then statistically compared. To reveal differences among the groups, one-way ANOVA followed by Tukey's test was used. The differences were considered significant at $P < 0.05$.

## 3. RESULTS

**Plasma Nanocoating and Surface Characterization.** The preparation conditions of plasma $SiO_x$:H nanocoating and surface characterization were summarized in Table 1. With the increase of oxygen ratio in the plasma system (the flow ratio of TMS was kept at 1 sccm in all groups), the water contact angle of the samples decreased from 98.5±2.3° to 26.3±4.0°. As the boundary of hydrophilicity and hydrophobicity, a contact angle of 65°, but not 90°, is widely accepted.[16] The original silicon wafers without $SiO_x$:H plasma nanocoating were not used as control in this study because of its different surface composition. With increase of the $O_2$ ratio in the plasma system, the deposited $SiO_x$:H coating exhibited gradually decreasing contact angle because of the increase of oxygen content in the deposited coating. The hydrophobic $CH_3$ function groups in TMS were replaced by hydrophilic oxygenous groups such as COOH, OH, or oxygenous free radicals. In this study, sample identification codes 1:0 and 1:1 ($TMS/O_2$ ratio; Table 1) groups were hydrophobic surface; 1:2 and 1:3 groups were neutral hydrophilic surface; 1:4 and 1:5 groups were hydrophilic surface, respectively. The thickness of all plasma coating was controlled at 30−40 nm on the smooth surface of silicon wafers by adjusting deposition duration. The composition and chemical states of the plasma $SiO_x$:H coating had been examined by X-ray photoelectron spectroscopy in our previous works.[14]

**Integrin Expression in Integrin-Rho GTPases Signaling Pathway.** It is well accepted that the protein absorption is the first event occurring at the interface of cells-biomaterials, which directly regulate subsequent cell adhesion.[17] The various information of surface determined ECM protein absorption, including FN, laminin (LN), vitronectin (VN), and Col, which bind to extracellular domains of integrin $\alpha$ subunits receptors on cell membrane, respectively. At first, the distribution and expression of FN mediated by surface wettabilities was investigated. It could be found from Figure 1 that FN was a dispersion distributed outside of cells on the surface of all groups, which provide sites for integrins binding and support cell body adhesion. 1:0−1:3 groups showed stronger fluorescent intensity than most hydrophilic surfaces (1:4 and 1:5 groups). The integrin $\alpha 2$ and $\alpha 5$ are primarily thought of as LN and FN receptor,[18] while $\alpha$V non-covalently connects intracellular domains of integrin $\beta 1$ and $\beta 3$ subunits as well, which are ligands of integrin cytoplasmic tails, playing a central role in binding and regulating the actin cytoskeleton to form FA complex and directly resulting in cell migration through sustained and transient signals.[19]

Integrin $\alpha V\beta 3$ has been proven to participate in a lot of cytokine-induced endothelial cell migration.[20,21] We examined the expression levels of integrin $\alpha$V, $\beta 1$, and $\beta 3$ in response to various wettabilities of plasma $SiO_x$:H nanocoating, respectively (the expressions of integrin $\alpha 2$ and $\alpha 5$ weren't shown, which were examined in our previous study). According to the comparative results (Figure 2a, b), the $\alpha$V subunit expression level of 1:5 groups was significantly higher than that of 1:3 and 1:4 groups. The 1:0 group (hydrophobicity more than 1:1 group) showed strongest expression level of integrin $\beta 3$, and hydrophobic surfaces (1:0 and 1:1 groups) and most

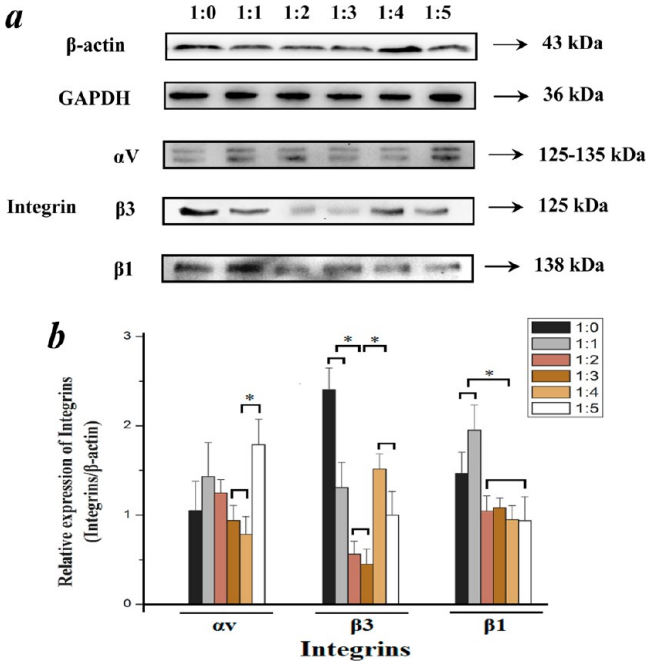


**Figure 2.** Effects of surface wettability on the expression of integrin subunits. (a) Representative Western blot of integrins expression. (b) Quantification of each integrin subunit's expression level by image analysis of the Western blot bands. The expression level of $\beta$-actin in each group was used as intrinsic controls, and relative expression of integrins were calculated. Values represent the mean±S.D. *, $P < 0.05$ denotes statistically significant difference compared with other groups.

hydrophilic surfaces (1:4 and 1:5 groups) revealed higher integrin $\beta 3$ compare to 1:2 and 1:3 groups with a neutral hydrophilic surface. However, only hydrophobic groups (1:1 and 1:0) showed higher expression of $\beta 1$ subunit in comparison with 1:2−1:5 groups. These differences suggested that integrins signals participated in surface wettability inducing cell adhesion and migration, and this process was not only restricted to one particular integrin receptor. Because of different ECM proteins adsorbed on plasma $SiO_x$:H nanocoatings with various wettabilities resulting in significant differences of integrins binding, it seemed that there was no obvious regularity about various integrin subunit expression.

**Associated Proteins of FA Complexes Expression.** Talin and paxillin are important ligands of $\beta$ integrin cytoplasmic tails. Talin plays a central role in the first step of focal complexes formation following initial integrin engagement, and talin degradation plays a critical role in FA turnover.[10] Vinculin, as a binding partner of talin, promotes and stabilizes initial integrin clustering. The effects of surface wettability on the expression of FA components (talin, vinculin, and paxillin) were examined in this study. It could be seen from Figure 3a, the expressions of talin and paxillin showed a similar increased trend from hydrophobic 1:0 samples to hydrophilic 1:4 groups, and decreased from 1:5 samples (Figure 3b). Interestingly, 1:5 samples showed high affinity for cell adhesion but significantly less in talin and paxillin expression levels compared with 1:4 groups. It is suggested that the surface performance of 1:5 groups experienced a marked alteration with the increased flow ratio of $O_2$ (to 5 sccm) or duration of plasma deposition (to 7 min), while the difference in contact angle was only about 3° and changes in components of Si, O, and C was less compared with 1:4 groups. The possible reason


dx.doi.org/10.1021/am400973a | ACS Appl. Mater. Interfaces 2013, 5, 5112−5121

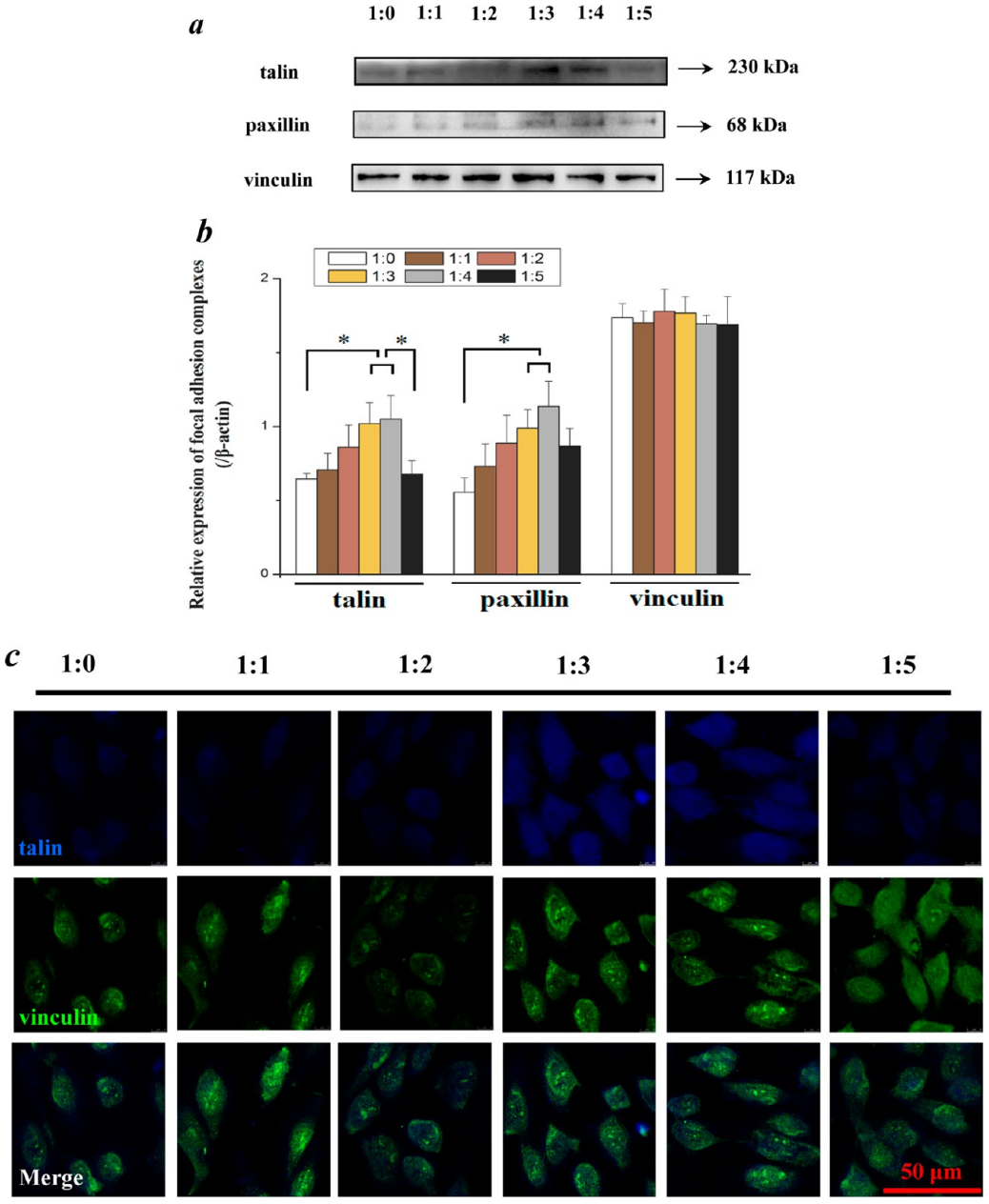


**Figure 3.** Effects of surface wettability on the expression and distribution of FA proteins by Western blot and immunofluorescence analysis. (a)Western blot analysis of the effects of plasma $SiO_x$:H surfaces with varying wettabilities on talin, paxillin, and vinculin protein expression. (b) Quantification of each FA components expression level by image analysis of the Western blot bands in panel (a). (c) The expression and distribution of talin (blue) and vinculin (green) on $SiO_x$:H surfaces by double immunofluorescent staining. Scale bar =50 $\mu$m.

is that the flow ratio of TMS and $O_2$ with 1:4 is saturated, and increased $O_2$ deposited on the surface as free radicals in plasma system. In this system, it was found that the increase of the flow ratio of $O_2$ (to 6 or 7 sccm) and deposited duration could hardly decrease contact angles. Meanwhile, the talin (blue) and vinculin (green) were mainly distributed in the whole cytoplasm, which supported cell body for adhesion and spreading (Figure 3c). However, there was no significant difference of vinculin expression among all samples (Figure 3b). These results suggested that increased surface wettability enhanced endothelial adhesion because more cytoskeletal proteins were recruited to form FA complexes, which could bind to ECM through integrins and support cell adhesion.

**Effects of Surface Wettability on Expression and Distribution of (*p*)FAK.** Cell migration dependent FAK-Rho GTPases signaling pathway has been indicated in previous studies.[11,12] FA formation has been shown to be accompanied by increasing phosphorylation of FAK. Figure 4a shows the expression and distribution of FAK and *p*FAK on $SiO_x$:H coating with various wettabilities by double immunofluorescence staining. According to the figures, the fluorescent intensities of total FAK in all groups were uniform, while the expression of *p*FAK in 1:0−1:2 groups showed higher fluorescent intensity compared to that on 1:3−1:5 groups, which was consistent with our previous Western blot result of FAK and *p*FAK.[14] The *p*FAK was evenly distributed in the whole cytoplasm, which coincided to the distribution of FAK. Merging the distribution of FAK and its phosphorylation, it could be clearly seen that, *p*FAK (green) expressed higher at the leading edge of the cell in 1:0 and 1:1 groups in comparison

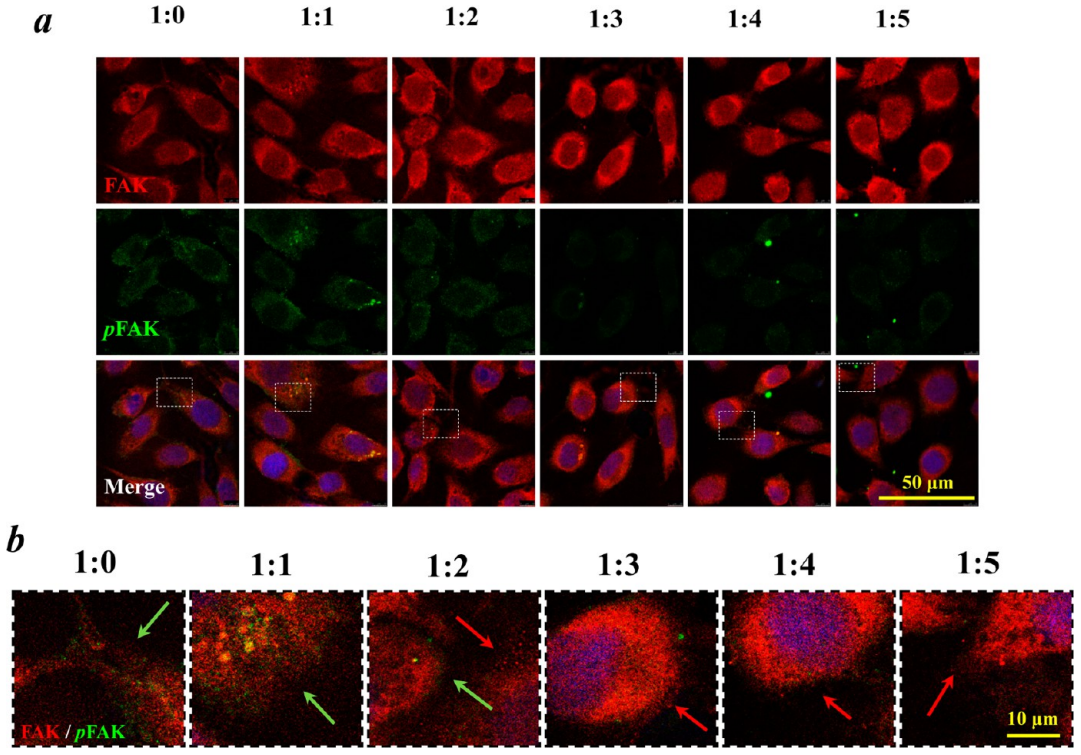


**Figure 4.** Effects of surface wettability on the expression and distribution of *t*FAK and *p*FAK. (a) Immunofluorescence analyses of the effects of $SiO_x$:H surfaces on protein expression of FAK (red) and *p*FAK(green). The nucleus is stained by DAPI (blue), marked in merged figures in panel (b). Scale bar = 50 $\mu$m. (b) Enlarged images of designated regions, indicated by white square frames in panel (a), the green arrows indicated clear distribution of phosphorylated FAK at the leading edge of cells in the hydrophobic surface, while in the hydrophilic surface (1:4 and 1:5 groups), the FAK with red fluorescence occupied the whole cytoplasm; less degree of green fluorescence could be observed at the cell periphery.

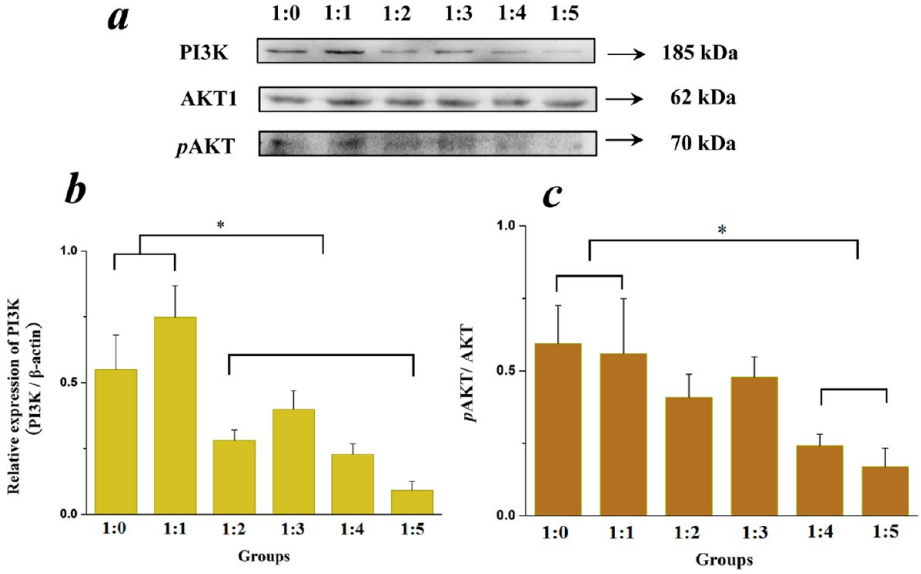


**Figure 5.** Effects of surface wettability on the protein expression of PI3K-(*p*)AKT signaling pathway. (a) Representative western blot bands of PI3K and (*p*)AKT. (b), (c) Quantification of PI3K expression level and the fraction of phosphorylated AKT in total AKT expression by image analysis of bands. *, $P < 0.05$ denoted statistically significant differences compared with other groups.

to 1:2-1:5 groups (Figure 4b are enlarged images of regions, indicated by white square frames in Figure 4a). Both the expression and the spatial distribution of (*p*) FAK suggested that hydrophobic surface could induce more phosphorylation of FAK, which lead to faster cell migration.

The autophosphorylation site in FAK at Y397 is a binding site for Src and PI3K, and PI3K-AKT signaling molecules are downstream of FAK in regulating cellular viability and migration.[12,22] Figure 5 showed the protein expressions of PI3K, total and phosphorylated AKT at threonine 308 site (*p*AKT). It could be seen from Figure 5a that the expression level of PI3K down-regulated with increase of wettability. There were significant differences between hydrophobic groups (1:0 and 1:1 groups) and the other four hydrophilic surfaces (1:2


dx.doi.org/10.1021/am400973a | ACS Appl. Mater. Interfaces 2013, 5, 5112−5121

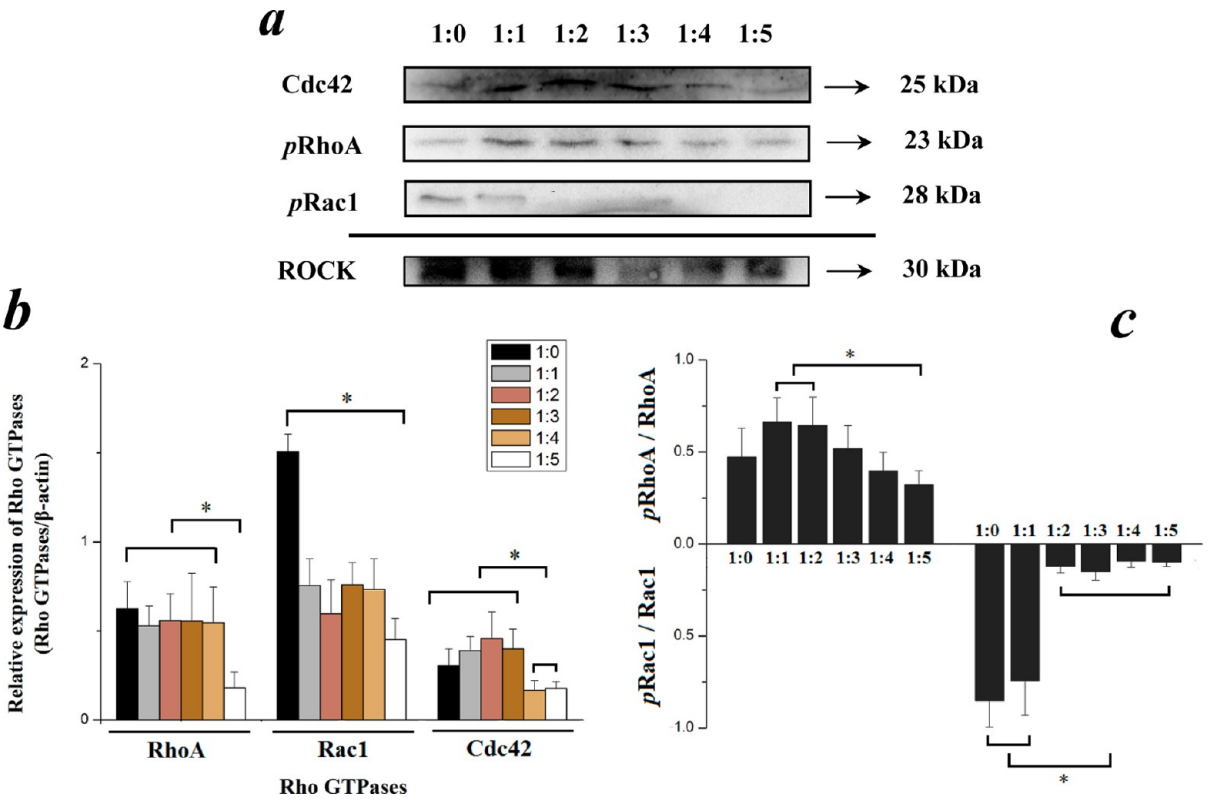


**Figure 6.** Effects of surface wettability on the expression of small G proteins and their phosphorylation level. (a), (b) Western blot analyses of the effects of varying surface wettabilities on *p*Rac1, *p*RhoA, Cdc42, and ROCK. The relative expression level of RhoA, Rac1, and Cdc42 were calculated and compared. (C) The ratio of phosphorylated RhoA (Rac1) in total RhoA (Rac1) was compared. *, $P < 0.05$ denoted statistically significant difference compared with other groups.

and 1:5 groups) (Figure 5b). We also found that all groups showed equal total AKT; however, hydrophobic groups (1:1 and 1:0 groups) showed higher expression of *p*AKT compared with most hydrophilic surfaces (1:4 and 1:5 groups, Figure 5c).

**Effects of Surface Wettability on the Expression and Distribution of Rho GTPases.** Our previous results showed equal expression level of RhoA in 1:0−1:4 samples, but to be down-regulated in 1:5 groups, and Rac1 was expressed highest in 1:0 and 1:1 groups, whereas lowest in 1:2 and 1:5 groups.[14] The Cdc42, which regulates filopodia also associated with cell migration, exhibited higher expression in 1:1−1:3 groups, but lower expression in 1:4 and 1:5 groups (Figure 6a). The relative expressions of RhoA, Rac1, and Cdc42 were calculated and depicted in Figure 6b. The immunofluorescence results of RhoA and Rac1 are shown in Supporting Information, Figure S1 a,b. Both immunofluorescent intensities of Rac1 and RhoA were consistent with results of western blot, and they revealed that Rac1 was mainly distributed in the cytoplasm while RhoA was distributed in both the cytoplasm and the nucleus. In addition, it could be found that the immunofluorescent intensity of Rac1 was lower in 1:2 and 1:5 groups in comparison to other groups (Supporting Information, Figure S1a), and results of RhoA showed obviously lower expression in 1:5 groups than that in other groups. Notably, it could be found that the distribution of RhoA in hydrophilic 1:5 groups dispersed expressed little in nucleus (white arrows in Supporting Information, Figure S1b), could hardly be observed in cytoplasm. Combined with previous result of FA components expression level (talin and paxillin), it is illustrated that most hydrophilic 1:5 groups promoted cell adhesion behavior in cellular level still showed an increased tendency (see Supporting Information, Figure S2), but the possible molecular mechanism was different compared with other groups. Furthermore, the phosphorylation level of RhoA at serine 188 (*p*RhoA) and Rac1 at serine 71 site (*p*Rac1) were examined in this study, and the ratio of phosphorylation levels (*p*RhoA and *p*Rac1) in total RhoA and Rac1 expressions were described in Figure 6c, respectively. The *p*RhoA in 1:1 and 1:2 groups was much higher than that in 1:5 groups, and *p*Rac1 was up-regulated in 1:0 and 1:1 samples (Figure 6a, c), which was consistent with our previous results of the cell migration study, namely, cells migrated faster on hydrophobic surfaces than on hydrophilic surfaces.[14]

In addition, Rho-associated protein kinase (ROCK) has been identified as key downstream effector of Rho GTPases and contributes to multiple cytoskeleton functions such as FAs and stress fibers, and phosphorylates myosin light chain (MLC) to induce actomyosin contractility for cell adhesion and migration. Based on Western blotting analysis, ECs showed elevated levels of ROCK in cells grown on the hydrophobic surfaces (1:0−1:2 groups) as compared to those on hydrophilic surfaces (1:3-1:5 groups) (Figure 6a). These results all demonstrated that hydrophobic surface could up-regulate Rho GTPases and ROCK, and result in enhancing ECs migration.

**Merged FA Proteins (talin) and Rho GTPases (Cdc42).** To further study the relationship between FA complexes and Rho GTPases, talin and Cdc42 were chosen to study respectively the distribution by double-labeled immunofluorescence analyses. As can be seen from Figure 7, the merged figures show that, the essential ingredient, cytoskeletal proteins talin was distributed more widely than Cdc42 in all groups (the expression levels of talin and Cdc42 in response to various

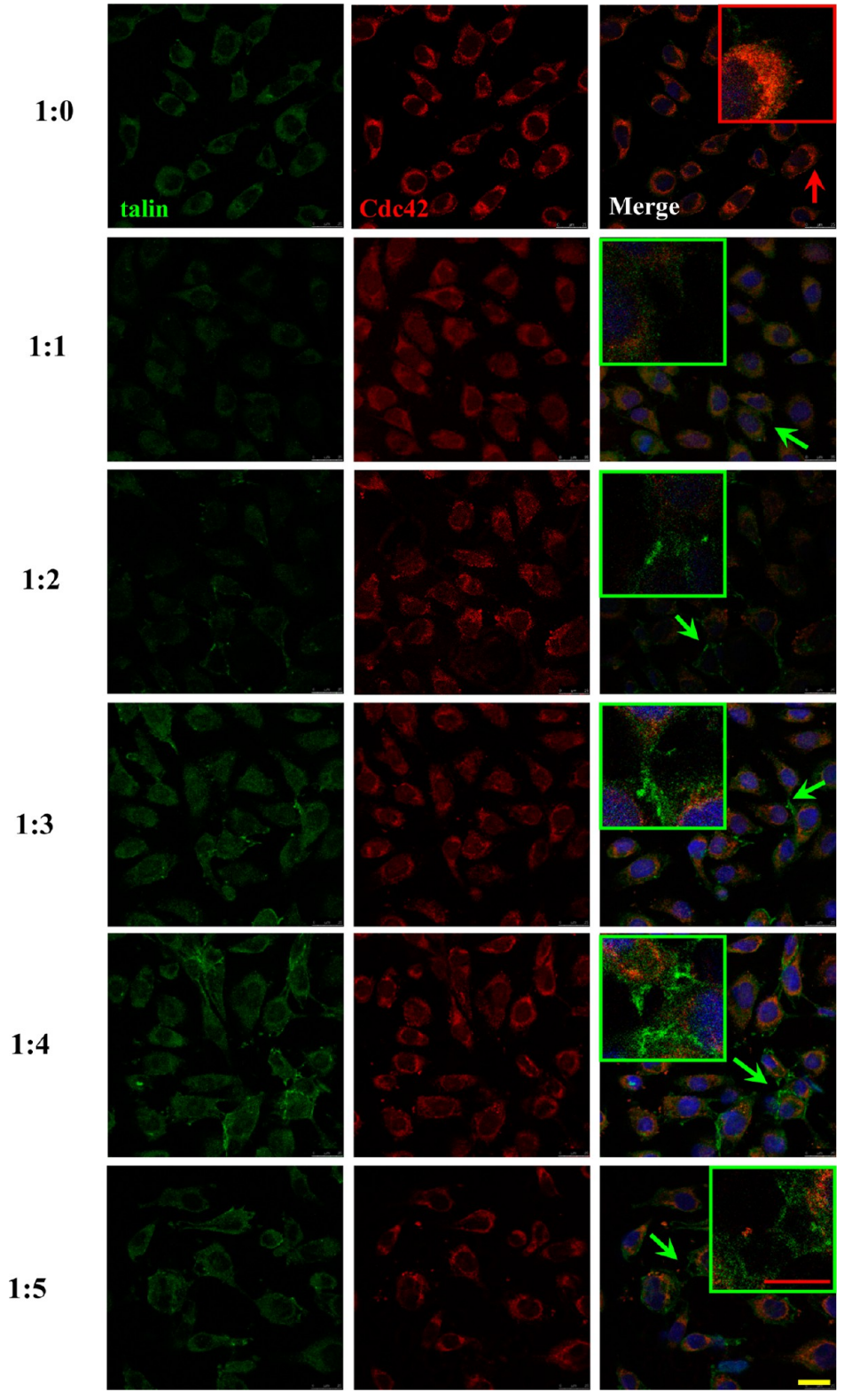


**Figure 7.** Double-labeled immunofluorescence analyzed the effects of varying surface wettabilities on distribution and expression of Cdc42 (red) and talin (green) proteins. (blue: DAPI stained nucleus). Yellow scale bar = 25 $\mu$m. The red arrows in figure (1:0 group) indicated red Cdc42 protein expressed stronger than green talin protein at the cell periphery in the merged figure, and the arrow designated region was enlarged and indicated by red square frames. While the green arrows in other figures indicated labeled green talin protein distributed wider than labeled red Cdc42 protein in 1:2-1:5 groups in merged figures, suggesting that hydrophilic surface (1:2-1:5 groups) could form broader focal adhesion regions to support cell adhesion, and the arrow designated region was enlarged and indicated by green square frames (red scale bar = 10 $\mu$m).

surface wettabilities have been identified and shown in previous Figure 3 and Figure 6, respectively). It could be obviously observed in hydrophilic 1:2−1:5 groups (green arrows in merged images in Figure 7), suggesting that hydrophilic surface


dx.doi.org/10.1021/am400973a | ACS Appl. Mater. Interfaces 2013, 5, 5112−5121

(1:2−1:5 groups) could form broader FA regions to support cell adhesion, accordingly enhancing cell spreading. It is consistent with our previous results of cellular adhered behavior that a hydrophilic surface could enhance cell adhesion. However, there is a difference of Cdc42 distribution among 1:0 groups and other groups. It could clearly found that, in 1:0 groups, Cdc42 proteins were mainly expressed at the edge of the cell body, while they were distributed in the whole cytoplasm in other groups (red arrows in merged images in Figure 7). No obvious intense green fluorescence (talin) was found at the leading edge of cells, suggesting that adhered cells on hydrophobic surface (1:0 groups) demonstrated a motive trend in favor of cell migration.

## 4. DISCUSSION

In this study, EA.hy 926 cells instead of primary endothelial cells were used because of their higher affinity to surfaces of materials. The EA.hy 926 cells, which retain most features and exhibit most phenotypes of HUVECs, express specific marker for endothelial cells in vitro including vWF and CD31, uptake of DiI-Ac-LDL.[23] This cell line was widely used to study cell adhesion and migration.[24,25] Actually, as selection of model cell type, the primary HUVECs purchased from ScienCell were initially considered and tested. However, HUVECs showed low affinity to surfaces without FN or collagen pre-coatings. In most available published similar works on studies of the interaction of cell-substrate, surfaces of materials must be coated with different FN for HUVEC culture.[26,27] Therefore, we choose EA.hy 926 cells in entire experiments, which could contact with plasma $SiO_x$:H nanocoating directly without FN induction. Under such circumstances, the distribution of adsorbed FN secreted from cells and expression level of integrins could be accurately studied, and it could better help us to describe the direct interaction between materials and cells because of higher affinity of EA.hy 926 cells to surfaces of materials.

Surface characteristics of implanted biomaterial, including wettability, energy, roughness, charge, and chemical composition, are all known to play central roles in regulating interaction between cells/tissue and biomaterials.[28] The self-assembled monolayers (SAMs) technique could be helpful to prepare the surface with well-controlled chemical functional groups. However, because of the introduction of hydrophilic (COOH, OH) or hydrophobic groups ($CH_3$), the surface wettability changed alone with surface chemistry. The modified surface with $CH_3$, $NH_2$, COOH, and OH groups by SAMs, contact angle were 107±1°, 43±3°, 28±1° and 25±3°, respectively.[29] Arima et al.[6] used different concentrations of terminal methyl ($CH_3$), hydroxyl (OH), carboxylic acid (COOH), and or amino ($NH_2$) groups (100/0, 75/25, 50/50, 30/70, 20/80, 10/90, 5/95, 0/100) to investigate protein adsorption and cell adhesion. Therefore, cells actually sense multiple information of material surface, induce cascaded activation of intracellular genes and proteins, and result in changes of their function and behavior.

Endothelial cell adhesion and migration is an essential process in angiogenesis, wound healing, vessel remodeling, and re-endothelialization. Nowadays, a lot of intercellular signaling pathways involving cell adhesion and migration are studied. Most researches mainly concentrate on integrins inducing phosphorylation of FAK and its downstream signaling events contributing to formation of stress fibers,[30] and vascular endothelial growth factor (VEGF) binding to its receptor (VEGFR2) to trigger activation of PI3K-AKT-eNOS or p38 MAPK pathway for cell proliferation and migration.[31] However, most of these studies were performed by using biochemical factors or mechanical stimulus, while few studies focused on surface properties of material induced cell signaling molecules, especially, a cascade transduction of one cellular signaling event. Using SAMs as model substrates, Kaselowsky et al.[26] proved that surface chemistry regulated $\alpha5\beta1$ integrin binding following the order OH > COOH═$NH_2$ > $CH_3$, and induced FAK phosphorylation at respective 576, 397, and 861 tyrosine site following the order $NH_2$ > OH═COOH > $CH_3$. Using MC3T3-E1 cells as well, Llopis-Hernandez' works indicated that both the gene and protein expression, the OH terminated SAMs showed higher level of *p*FAK, matrix metalloproteinases (MMP-2 and MMP-9) and RUNX2 compared with 30, 50, 70, and 100% $CH_3$ groups.[32] As a whole, their studies suggested that the hydrophilic functional group (OH and COOH) resulted in higher expressions of integrins and (*p*)FAK, which is not consistent with our conclusion, suggesting that a variety of cell types respond differently to surface wettability. Using other model substrates, Hung et al.[33,34] demonstrated VEGFR2-PI3K-Akt-eNOS-NO signaling pathways were associated with ECs proliferation and migration on polyurethane nanocomposites. In addition, using osteoblastic cells as model cell, Kim et al. demonstrated that Rho-associated kinase (ROCK) inhibitor could significantly enhance adhesion, migration, and proliferation of osteoblastic cells cultured on a hydrophobic polystyrene surface ($\theta \approx 85°$),[35] and very recently they have emphasized the RhoA-ROCK-PTEN pathway as a molecular switch for anchorage dependent cell adhesion and proliferation on the hydrophilic and hydrophobic substrates.[36] It could be seen from the above studies that selecting different cells type and various material surfaces would find inconsistent conclusions. In the present study, the cascade response of protein expression in integrin-FAK-Rho GTPases pathway was performed, and the results indicated that the hydrophilic surface exhibited higher cytoskeletal proteins (talin and paxillin) to form the FA complex, which are possible reasons why hydrophilic surface could enhance ECs adhesion; whereas hydrophobic surface showed higher *p*FAK and small G proteins expression, which are possible reasons why hydrophobic surface could promote ECs migration.

The FA's formation directly impact on the adhesive strength of cells on the material surface, and regulates cell adhesion and migration. Our previous study demonstrated that hydrophilic plasma $SiO_x$:H coating promoted endothelial cell adhesion, whereas hydrophobic surface enhanced cell migration.[14] Our results in this study further confirmed the molecular mechanisms that FA complexes associated with cell adhesion (talin, and paxillin) were expressed relatively higher with respect to hydrophilic surface. Therefore, the behaviors of cell adhesion and migration are likely opposite because of formation of FAs and presence of adhesion strength.

In this study, the duration of cell adhesion at 48 h was chosen for both western blot and immunofluorescence analysis. Under such circumstances, cells in all groups showed 60−80% confluence, enough that firm FA was formed, and there was residual surface space for cell spreading and migration (See Supporting Information, Figure S2). It should be noted that, the protein expression should be different when cells sense surface wettability at the initial stage. Therefore, it is significant to explore the changing of intracellular signaling events with increase of contact duration.

## 5. CONCLUSIONS

In this study, the expression and distribution of the relative crucial proteins in integrin-FAs-(*p*)FAK-PI3K-(*p*)AKT-Rho GTPases signaling pathway in response to plasma $SiO_x$:H nanocoatings with well-controlled surface wettability were examined. We found that multiple subunits of integrins showed irregular expression because of the complexity of deposited ECM proteins on the surface of biomaterials. As important ligands of $\beta$ integrin cytoplasmic tails, FA complex (talin, paxillin) showed a higher expression on hydrophilic surface, which is consistent with adhesion behavior at the cellular level, while hydrophobic surface enhanced the expression of (*p*)FAK, PI3K, (*p*)AKT, Rho GTPases, and ROCK, which suggests a stepwise activation of signaling cascades for cell migration. It could be obviously discovered when overlapping the FAs and Rho GTPases by double immunofluorescence staining (Figure 7). Understanding the relationship of the molecular mechanism of surface properties regulating cell adhesion/migration could guide the surface modification of implants, which is expected to design a proper surface for balancing cell adhesion and migration and achieving rapid endothelialization.

## ■ ASSOCIATED CONTENT

### Ⓢ Supporting Information

Figures showing the effects of various surface wettabilities on the distribution of Rac1 and RhoA (Figure S1) and the cell density (Figure S2) after 48 h culture. This material is available free of charge via the Internet at http://pubs.acs.org.

## ■ AUTHOR INFORMATION

### Corresponding Author

*E-mail: liuxiaohg@scu.edu.cn.

### Author Contributions

‖These authors contributed equally to this work.

### Notes

The authors declare no competing financial interest.

## ■ ACKNOWLEDGMENTS

This study was supported in part by grant from National Natural Science Foundation of China (No.11172198, 10972148, and 50830102), Visiting Scholar Foundation of Key Laboratory of Biorheological Science and Technology (Chongqing University), Specialized Research Fund for the Doctoral Program of Higher Education (20120181120058) and China Medical Board (82-412).

## ■ REFERENCES

(1) Saito, T.; Hokimoto, S.; Oshima, S.; Noda, K.; Kojyo, Y.; Matsunaga, K. *Cardiovasc. Revasc. Med.* **2009**, *10* (1), 17−22.
(2) Versari, D.; Lerman, L.O.; Lerman, A. *Curr. Pharm. Des.* **2007**, *13* (17), 1811−1824.
(3) Ball, M.; Grant, D.M.; Lo, W.J.; Scotchford, C.A. *J. Biomed. Mater. Res. A* **2008**, *86A* (3), 637−647.
(4) Pelliccia, F.; Cianfrocca, C.; Rosano, G.; Mercuro, G.; Speciale, G.; Pasceri, V. *JACC Cardiovasc. Interv.* **2010**, *3* (1), 78−86.
(5) Watt, S.M.; Athanassopoulos, A.; Harris, A.L.; Tsaknakis, G. *J. R. Soc. Interface* **2010**, *6*, S731−751.
(6) Arima, Y.; Iwata, H. *Biomaterials* **2007**, *28* (20), 3074−3082.
(7) Saravia, V.; Toca-Herrera, J.L. *Microsc. Res. Technol.* **2009**, *72* (12), 957−64.
(8) Tzoneva, R.; Faucheux, N.; Groth, T. *Biochim. Biophys. Acta* **2007**, *1770* (11), 1538−1547.
(9) Parsons, J.T.; Horwitz, A.R.; Schwartz, M.A. *Nat. Rev. Mol. Cell. Biol.* **2010**, *11* (9), 633−643.
(10) Wiesner, S.; Legate, K.R.; Fassler, R. *Cell Mol. Life Sci.* **2005**, *62* (10), 1081−1099.
(11) Wozniak, M.A.; Modzelewska, K.; Kwong, L.; Keely, P.J. *BBA-Mol. Cell. Res.* **2004**, *1692* (2-3), 103−119.
(12) Cain, R.J.; Ridley, A.J. *Biol. Cell.* **2009**, *101* (1), 13−29.
(13) Mitra, S.K.; Hanson, D.A.; Schlaepfer, D.D. *Nat. Rev. Mol. Cell. Biol.* **2005**, *6* (1), 56−68.
(14) Shen, Y.; Wang, G.X.; Huang, X.L.; Zhang, Q.; Wu, J.; Tang, C.J.; Yu, Q.S.; Liu, X.H. *J. R. Soc. Interface.* **2012**, *9* (67), 313−327.
(15) Kim, M.S.; Shin, Y.N.; Cho, M.H.; Kim, S.H.; Kim, S.K.; Cho, Y.H.; Khang, G.; Lee, I.W.; Lee, H.B. *Tissue Eng.* **2007**, *13* (8), 2095−2103.
(16) Vogler, E.A. *Adv. Colloid Interface Sci.* **1998**, *74*, 69−117.
(17) Kasemo, B.; Gold, J. *Adv. Dent. Res.* **1999**, *13*, 8−20.
(18) Belkin, A.M.; Stepp, M.A. *Microsc. Res. Tech.* **2000**, *51* (3), 280−301.
(19) Moissoglu, K.; Schwarz, M.A. *Biol. Cell.* **2006**, *98* (9), 547−555.
(20) Mikelis, C.; Sfaelou, E.; Koutsioumpa, M.; Kieffer, N.; Papadimitriou, E. *FASEB. J.* **2009**, *23* (5), 1459−1469.
(21) Gao, B.; Saba, T.M.; Tsan, M.F. *Am. J. Physiol. Cell Physiol.* **2002**, *283* (4), C1196−1205.
(22) Xia, H.; Nho, R.S.; Kahm, J.; Kleidon, J.; Henke, C.A. *J. Biol. Chem.* **2004**, *279* (31), 33024−33034.
(23) Unger, R.E.; Krump-Konvalinkova, V.; Peters, K.; Kirkpatrick, C.J. *Microvasc. Res.* **2002**, *64* (3), 384−397.
(24) Komorowski, J.; Jerczyńska, H.; Siejka, A.; Barańska, P.; Ławnicka, H.; Pawłowska, Z.; Stepień, H. *Life Sci.* **2006**, *78* (22), 2558−2563.
(25) Vrekoussis, T.; Stathopoulos, E.N.; De Giorgi, U.; Kafousi, M.; Pavlaki, K.; Kalogeraki, A.; Chrysos, E.; Fiorentini, G.; Zoras, O. *J. Chemother.* **2006**, *18* (1), 56−65.
(26) Keselowsky, B.G.; Collardm, D.M.; Garcia, A.J. *Biomaterials* **2004**, *25* (28), 5947−5954.
(27) Lan, M.A.; Gersbach, C.A.; Michael, K.E.; Keselowsky, B.G.; Garcia, A.J. *Biomaterials* **2005**, *26* (22), 4523−4531.
(28) Anselme, K.; Bigerelle, M. *Biomaterials* **2006**, *27* (8), 1187−1199.
(29) Keselowsky, B.G.; Collard, D.M.; Garcia, A.J. *J. Biomed. Mater. Res. A* **2003**, *66* (2), 247−259.
(30) Berrier, A.L.; Yamada, K.M. *J. Cell Physiol.* **2007**, *213* (3), 565−573.
(31) Lamalice, L.; Le Boeuf, F.; Huot. *J. Circ. Res.* **2007**, *100* (6), 782−794.
(32) Llopis-Hernandez, V.; Rico, P.; Ballester-Beltran, J.; Moratal, D.; Salmeron-Sanchez, M. *PLoS One.* **2011**, *6* (5), e19610.
(33) Hung, H.S.; Wu, C.C.; Chien, S.; Hsu, S.H. *Biomaterials* **2009**, *30* (8), 1502−1511.
(34) Hung, H.S.; Chu, M.Y.; Lin, C.H.; Wu, C.C.; Hsu, S.H. *J. Biomed. Mater. Res. A* **2012**, *100* (1), 26−37.
(35) Tian, Y.S.; Kim, H.J.; Kim, H.M. *Biochem. Biophys. Res. Commun.* **2009**, *386* (3), 499−503.
(36) Yang, S.; Kim, H.M. *Biomaterials* **2012**, *33* (10), 2902−2915.